ACS APPLIED MATERIALS & INTERFACES

Letter

www.acsami.org

DNA-Assisted β-phase Nucleation and Alignment of Molecular Dipoles in PVDF Film: A Realization of Self-Poled Bioinspired Flexible Polymer Nanogenerator for Portable Electronic Devices

Abiral Tamang,[†,‡] Sujoy Kumar Ghosh,[†,‡] Samiran Garain,[‡] Md. Mehebub Alam,[‡] Jörg Haeberle,[§] Karsten Henkel,[§] Dieter Schmeisser,[§] and Dipankar Mandal*[,‡]

[‡]Organic Nano-Piezoelectric Device Laboratory, Department of Physics, Jadavpur University, Kolkata 700032, India

[§]Angewandte Physik-Sensorik, Brandenburgische Technische Universität Cottbus-Senftenberg, K.-Wachsmann-Allee 17, 03046 Cottbus, Germany

Supporting Information

ABSTRACT: A flexible nanogenerator (NG) is fabricated with a poly(vinylidene fluoride) (PVDF) film, where deoxyribonucleic acid (DNA) is the agent for the electroactive β-phase nucleation. Denatured DNA is co-operating to align the molecular $-CH_2/-CF_2$ dipoles of PVDF causing piezoelectricity without electrical poling. The NG is capable of harvesting energy from a variety of easily accessible mechanical stress such as human touch, machine vibration, football juggling, and walking. The NG exhibits high piezoelectric energy conversion efficiency facilitating the instant turn-on of several green or blue light-emitting diodes. The generated energy can be used to charge capacitors providing a wide scope for the design of self-powered portable devices.

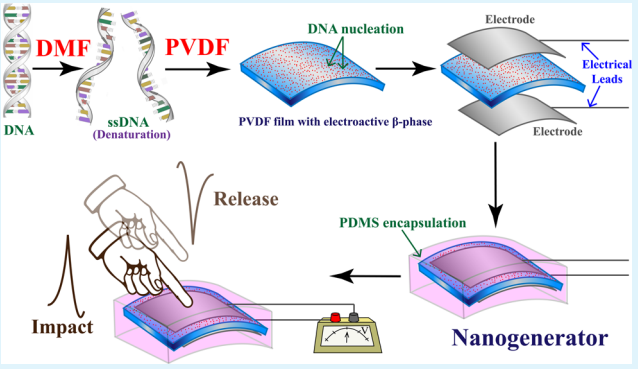

KEYWORDS: *PVDF, β-phase, DNA, self-poling, piezoelectric flexible nanogenerator*

Self-powered flexible mechanical energy harvesters such as nanogenerators (NG) have gained considerable attention because of the increased use of portable and biodegradable electronic devices caused by the increased mobility in human life style.[1−5] The importance of portable nanogenerators is also focused by the growing need of alternative energy sources.[3−8]It has been expected that piezoelectric based NGs can play a significant role for embedded electronic systems and biomedical sensors fabrication where the need of external power sources may be ignored.[9,10] However, the brittleness, weight, flexibility, and biocompatibility limit the use of inorganic based NGs, especially in embedded *in vivo* self-powered device realizations. In this context, lightweight polymer materials are attractive. PVDF can be considered as one of the most important semicrystalline polymers that have tremendous potential for the development of advanced materials. Flexible films made with PVDF have the highest attraction due to its biocompatibility, chemical resistance, good film forming capability, cost-effectiveness and brilliant electroactive properties viz. piezo-, pyro-, and ferroelectricity.[11] PVDF has four different crystalline phases (*viz*, α, β, γ, and δ) depending on the stereochemical macromolecular confirmations. The α-phase ($TGTG'$ confirmation) with alternating trans (T) and gauge (G) linkage is the most common electrically inactive nonpolar phase. Among the other phases that are electrically active polar phases, the β ($TTTT$ confirmation) phase is of greater importance, as it exhibits large spontaneous polarization and piezoelectric sensitivity. Because of these desired properties, tremendous efforts have been paid to induce the electroactive β-phase in PVDF. However, typically, piezoelectric activity cannot be registered until the PVDF layer is placed into an electric field which aligns the randomly oriented molecular CH_2/CF_2 dipoles along the electric field direction (called electrical poling).[12] Electric poling is not always desirable as it requires substantial power expenditure, electrical breakdown failure often occurs and it may also not be practical for specific use where certain desirable shapes are required such as for skin sensors, robotic interface, etc.[13,14] Over the years, many different techniques have been used to substitute the electrical poling in the β-phase containing PVDF films such as nanoparticle doping, hydrated salt film, and Langmuir−Schaefer methods where the use of typical poling-steps was avoided.[1,2,15]

In this work, we have doped the PVDF matrix with condensed nanostructured DNA to prepare self-poled β-phase containing PVDF films and to subsequently fabricate flexible NGs based on these films. DNA is a complex biopolymer with promising physical and electrical properties.

Received: May 13, 2015
Accepted: July 20, 2015
Published: July 20, 2015

DOI: 10.1021/acsami.5b04161
ACS Appl. Mater. Interfaces 2015, 7, 16143−16147

Because of its well-defined shape and electrical properties, DNA can be useful for the fabrication of advanced materials. The negative charge on the surface of the DNA arising from the phosphate backbone can be employed for the β-phase nucleation in PVDF. Single-strand DNA (ssDNA) is electrically of more interest as the nucleotide bases are exposed which can lead to interaction by H-bonding with suitable new materials such as PVDF. By selecting DNA as nucleating agent of the piezoelectric β-phase in PVDF a complete biodegradable system can be realized. In addition, DNA as nucleating agent has the advantage over hydrated salts and nanoparticles because of its biocompatibility and nontoxic nature. We have observed that the DNA-mediated PVDF film exhibits ultrasensitive pressure response and dipole reversibility due to the local ordering of the molecular dipoles. It signifies that an additional electrical poling step is not necessary for complete molecular dipole ordering. Thus, the DNA molecule can serve as an assisting agent for the activation of the electroactive phases in PVDF, which can provoke the fabrication of energy generators and smart sensors with altering ferro-, piezo-, and pyroelectric properties.

DNA in TE buffer solution (5 μg/mL, pH 8.0) was lyophilized. Then, 10 mL of 6 wt % (w/v) PVDF-DMF solution was poured into the lyophilized DNA container. The films were prepared by solution casting process on clean glass substrates and subsequently dried at 60 °C for 5 h. A reference (pure) PVDF-DMF film was also prepared for comparison. Finally, free-standing flexible films (Figure 1a) were achieved by peeling them from the glass substrates and were labeled as "Neat PVDF" (where no additive is present) and "DNA-PVDF" (where the calf thymus DNA is utilized). The fabrication of piezoelectric NG is discussed in the experimental section of the Supporting Information.

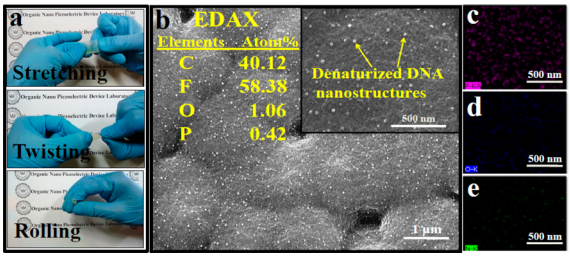

Figure 1. (a) Flexible nature of the DNA-PVDF film is demonstrated by stretching, twisting and rolling the film. (b) FE-SEM images of DNA-PVDF composite film with the inset displaying the higher magnified view and atomic % of carbon, fluorine, oxygen, and phosphor. (c–e) Element mapping images of phosphor, oxygen, and nitrogen, respectively.

Field-emission scanning electron microscopy (FE-SEM, INSPECT F50, FEI) images reveal that the DNA condenses into spherical nanostructured shapes over the PVDF matrix (Figure 1b). This is due to the fact that DNA denatures in DMF and then single strand DNA condenses to form nanostructured spheres.[5,16] The average size of these DNA condensates ranges between 30 and 45 nm in diameter. The elemental quantification performed using energy-dispersive X-ray (EDX, Bruker Nano X-flash detector, 410-M) shows the appearance of phosphor and oxygen in the film which could originate from the DNA presence (left inset of Figure 1b). The fluorine signal is arising from the PVDF molecule and carbon is mainly due to PVDF and might be from the dopant amount of DNA as well. The element mapping (Figure 1c–e) also reveals the presence of nitrogen (along with phosphor and oxygen) in the film, which was not obtained by EDX element quantification.

Fourier transform infrared spectroscopy (FT-IR, 8400S, Shimadzu) of our films clearly shows the nucleation of the fully polar β-phase in the DNA-PVDF composite film, as evident from the appearance of the intense vibrational band at 1273 cm^{-1}, which is not present in the Neat PVDF film (Figure 2a). The semipolar γ-phase is present in both the Neat PVDF and the DNA-PVDF composite films as evident from the 1234 cm^{-1} peak; however, it gets reduced because of the β-phase nucleation in the composite film.

The dual character peaks (β and γ-phases) at 509 and 840 cm^{-1} also indicate the β-phase formation in the DNA-PVDF composite film. The peak at 509 cm^{-1} is much more intense in the DNA-PVDF composite film supporting the nucleation of the β-phase in addition to the γ-phase. The peak at 837 cm^{-1} present in the Neat PVDF film is due to γ-phase and it gets intensified to a peak at 841 cm^{-1} in the DNA-PVDF film also suggesting that the β-phase has been induced (~80% relative proportion) (see the Supporting Information, Figure S1) in the composite. At the higher frequency region of the FT-IR spectra, shown in Figure 2b, two distinct vibrational bands are evident, assigned as asymmetric (ν_{as}) and symmetric (ν_s) vibrational modes of $-CH_2$ groups present in PVDF. Gaussian curve fitting (inset of Figure 2b) of the 3020 cm^{-1} (ν_{as}) peak shows a shift in the peak position of the DNA-PVDF film compared to the Neat PVDF film. This peak shift corresponds to interfacial interactions arising from negative surface charges of the DNA (σ_{eff}^{-}) and the $-CH_2$ dipoles (δ_{eff}^{+}) of the PVDF (Scheme 1).

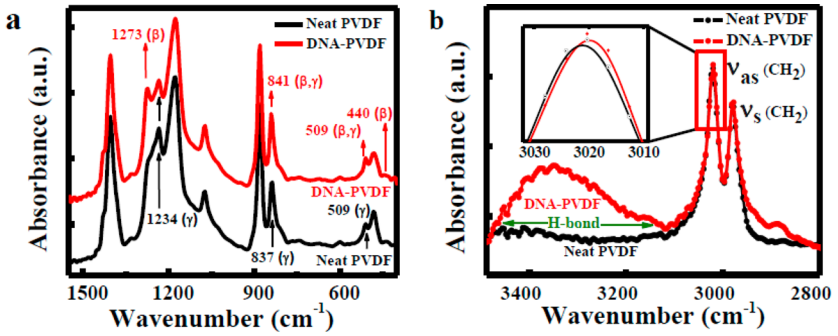

Figure 2. FT-IR spectra of Neat PVDF and DNA-PVDF composite in (a) 1550–400 cm^{-1} and (b) 3500–2800 cm^{-1} regions. The inset in part b shows the enlarged view of the best fitting of the asymmetric (ν_{as}) stretching vibrational mode peak.

DOI: 10.1021/acsami.5b04161
ACS Appl. Mater. Interfaces 2015, 7, 16143–16147

Scheme 1. Schematic Diagram Showing DNA Denaturation in DMF and Subsequent Formation of DNA-PVDF Film[a]

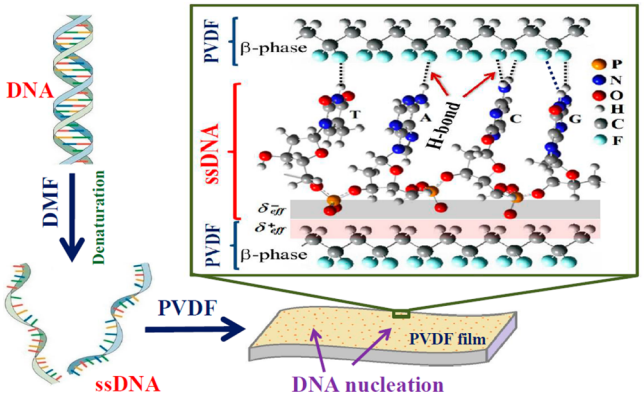

[a]The enlarged figure shows the ionic interaction between the ssDNA phosphate backbone and hydrogen bonding from the exposed DNA bases with molecular dipoles (CH_2/CF_2) of PVDF chains for the stabilization of the β-crystalline phase. A (adenine), T (thymine), G (guanine), and C (cytosine) represent the bases of the ssDNA molecule.

It has been reported above that DNA denatures in the presence of DMF, giving ssDNA, which condensates into spherical nanostructures.[16] The nanospheres could be negatively charged on the outer surface if the phosphate backbone of the ssDNA is toward the surface of the sphere, whereas in other cases, the surface of these ssDNA spheres could have the exposed bases forming H-bonds at the surface. A broad peak appears in the 3480−3120 cm^{-1} region within the FT-IR spectrum of the DNA-PVDF composite film, signifying that H-bond formation has occurred.[17] It is noteworthy that a broadening of this peak occurs because of the variation of the microenvironments of the ground state of the −OH stretching vibration.[18,19]

In addition to the negative charge on the phosphate backbone of the DNA, (i.e., ssDNA) the nucleotide bases may have strong affinity to the formation of H-bonds with the $-CF_2$ dipoles of PVDF (Scheme1). The H-bond formation could be crucial for the orientation of the $-CH_2$ and $-CF_2$ dipoles, leading to the self-poled β-phase formation that has a direct impact on the spontaneous piezoelectricity generation, where external electrical poling steps can be avoided.

For a better understanding of the compositional changes in the PVDF films in the presence of DNA, X-ray photoelectron spectroscopy (XPS) was carried out with monochromatic Mg K_α ($h\nu \sim 1253.6$ eV) excitation source and Omicron-EA925 analyzer on both, Neat PVDF and DNA-PVDF films. From the high resolution F 1s core level spectra an asymmetry can be seen in the data of the DNA-doped PVDF film in comparison to the Neat PVDF film (Supporting Information, Figure S2). The corresponding broadening of the peak reflects a change in the peak area ($\Delta A_{F\ 1s}$) of ∼3.1%. The peak broadens on both sides of the peak maximum position at −688.1 eV with larger asymmetry on the higher binding energy side. This result supports the fact that interfacial interactions between the DNA molecules and the CH_2/CF_2 dipoles of the PVDF film occur. The high-resolution C 1s core level spectrum of the Neat PVDF film shows two peaks contributed by the two main carbon species, i.e., CH_2 and CF_2, with binding energies of −289.9 and −294.3 eV, respectively (Figure 3a). However, in the data of the DNA-PVDF composite film, these peaks show major shifts toward lower binding energies, where the CH_2 and

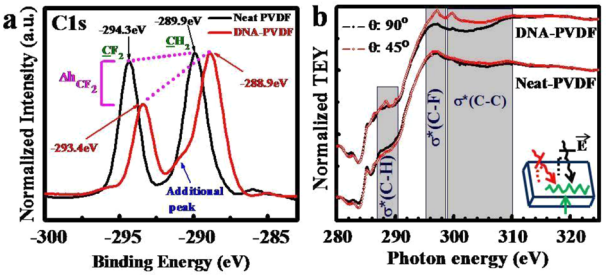

Figure 3. (a) C 1s core level XPS spectra of Neat-PVDF and DNA-PVDF films. The data are normalized to the highest intensity inside each spectrum. (b) NEXAFS normalized intensity at the C−K edge for Neat-PVDF and PVDF-DNA films.

CF_2 peaks appear at −288.9 and −293.4 eV, respectively. These binding energy shifts suggest that the electronic environment of the CH_2 and CF_2 dipoles of PVDF has changed considerably in the presence of DNA.

An additional peak broadening with a distinct shoulder at −291.1 eV is observed in between the binding energies of the CH_2 and CF_2 species in the C 1s data of the DNA-PVDF film. This is further evidence that there are interfacial interactions between the CH_2/CF_2 - dipoles of PVDF and the charged surface of the DNA molecules. A substantial intensity difference in the CF_2 peaks (Δh_{CF_2}) is obtained when the spectra are normalized to the CH_2 peaks. The DNA-PVDF sample exhibits a 31.6% reduction in the peak area of the CF_2 species (ΔA_{CF_2}) and an increase of 18.6% in the peak area attributed to the CH_2 species (ΔA_{CH_2}), which strongly indicate interfacial interactions.[20−22]

The angular dependent Near Edge X-ray Absorption Fine Structure (NEXAFS) total electron yield (TEY) was measured at the undulator beamline U49/2-PGM2 at BESSY-II, Germany equipped with the ASAM end station.[23,24] The NEXAFS normalized intensity in three distinct resonance regions, i.e., σ^* (C−H), σ^* (C−F), σ^* (C−C) in the C−K edge spectra of the PVDF-DNA film (Figure 3b) exhibit prominent intensity differences when X-ray excitation was done at two different incidence angles, signifying the local orientation of the CH_2/CF_2 dipoles.[25,26] In contrast, no significant polarization dependence is found in the C−K edge data of Neat PVDF film due to the randomly oriented dipoles.

The piezoelectric response of the NG in terms of open circuit voltage (V_{oc}) (Figure 4a) and short circuit current (I_{sc}) (measured through a full wave bridge rectifier) were recorded with digital oscilloscope (DS03102A, Agilent) and picoammeter (DPA-111, Scientific Instruments, Roorkee) (Supporting Information Video S1). The NG is highly sensitive to human touch as demonstrated in Supporting Information Video S1. A human finger touch response generates V_{oc} and I_{sc} values of 6 V and 0.088 μA, respectively, when the applied stress (σ_a) was 13 kPa (Figure 4a). Furthermore, when σ_a was increased to 63 kPa these values increased too (20 V, 0.184 μA). Simulations of the generated piezoelectric potential distribution in the NG with the DNA-PVDF film as the active element under an axial stress of 63 kPa were performed via finite element method (FEM) using COMSOL multiphysics software. The piezopotential distribution is presented by color code with z-axial mechanical stress (inset, Figure 4a). Similar results with output pulse voltages in the reversed direction were achieved in the human finger touch response experiments when reversing the polarity

DOI: 10.1021/acsami.5b04161
ACS Appl. Mater. Interfaces 2015, 7, 16143−16147

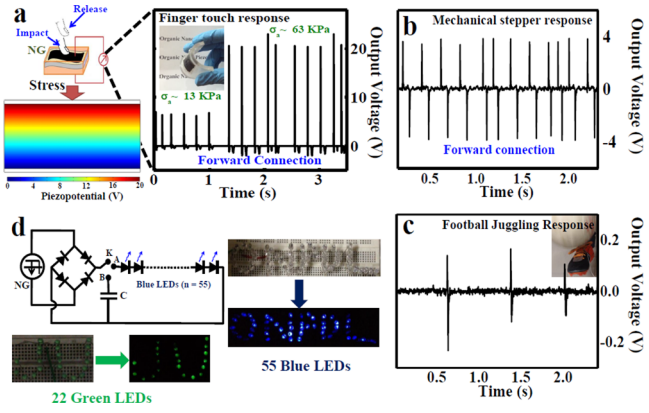

Figure 4. Touch responses of the DNA-PVDF film in forward connection when subjected to (a) finger patting with lower ($\sigma_a \approx 13$ kPa) and higher ($\sigma_a \approx 63$ kPa) mechanical stress. The inset on the bottom left corner denotes simulated induced piezopotential distribution inside the DNA-PVDF film under compressive normal stress of 63 kPa via finite element method (FEM), (b) mechanical stepper (stepper motor probe of portable sewing machine), and (c) football juggling when the NG was placed on top of football boots. (d) Simplified circuit diagram to demonstrate the illumination of LEDs (when K was connected with A) and capacitor charging (when K was connected with B) using the NG. In addition the illumination of green or blue LEDs (22 or 55 respectively) driven by the touch response of NG is shown.

of the NG leads (Supporting Information, Figure S3). This result is an indirect proof of the dipole reversibility that arises because of the alignment of the CH_2/CF_2 dipoles, as also evident from the NEXAFS results reported above (Figure 3b). Similar performances were observed for several mechanical stress responses. For example machine vibration was detected, where the NG was subjected to the periodic impact from the probe of a sewing machine (Figure 4b, Supporting Information, Video S1). In addition, football juggling response was demonstrated by strapping the NG on top of the boots with electrical leads connected to the oscilloscope where the impact of the football produced a pulsed output voltage response (Figure 4c, Supporting Information, Video S1). Furthermore, the NG was placed on the floor and was stimulated by walking step simulation to produce an output voltage signal that could be unique for individuals (Supporting Information, Video S1). Furthermore, the NG shows substantial output performance when repeatedly bent and released by human finger which also exhibits the tremendous flexibility (Supporting Information, Figure S4). To demonstrate the energy generating capability of the NG, 55 blue LEDs and in a different setup, 22 green LEDs were directly connected in series with the output leads of the NG as shown in Figure 4d and the Supporting Information, Video S1. Finger touch responses showed that the sensor is capable of turning on these LEDs paving a way to a suitable application of the sensor as an electric generator. We have observed that the voltage signal across a resistance generated by the NG increases gradually with the value of the resistance and saturates at a very high resistance, which corresponds in principle to the open circuit condition (Figure 5a). The instantaneous output power density of the NG gives a maximum of 11.5 $\mu W/cm^2$ at a resistance of 9 MΩ. Thus, it is evident that DNA doped PVDF films can serve as excellent flexible piezoelectric energy generators without any electric poling requirement. Furthermore, it should be noted that a poled Neat PVDF film generates significantly reduced power in

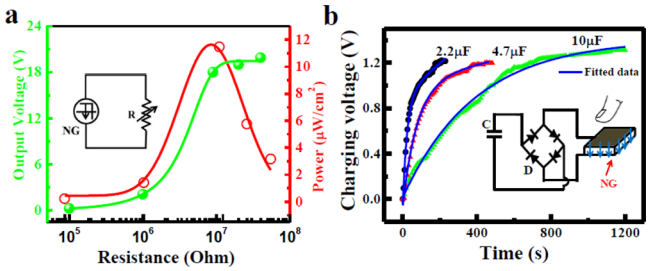

Figure 5. (a) Output voltage and power across varying resistances generated from NG by touch response (inset shows the circuit used). (b) Transient response of capacitors charging using the pulsed output generated from the NG driven by repeated finger touches. The inset shows the used bridge rectifier circuit.

comparison with our results.[27] The transient response of capacitance charging with the NG was investigated with a typical bridge wave rectifier circuit (inset of Figure 5b). Capacitors (2.2, 4.7, and 10 μF) were charged by applying stress on the NG and it was evident that the accumulated voltage rises exponentially and reaches a steady state (Figure 5b). The maximum energy harvesting efficiency (η_{NG}) was observed to be 2.7% (Supporting Information, Table S1), which is an improvement compared to the earlier works where the similar measurement system was used.[28−30] By effectively charging capacitors, we have demonstrated that mechanical energy can be easily harvested by the piezoelectric behaving DNA-PVDF film.

Flexible DNA-PVDF films are prepared by a simple solvent casting method and are completely biodegradable. The nucleation of the electroactive β- and γ- phases are obtained and intensified by the presence of the ssDNA without any electrical poling. This phenomenon can be explained by the electrostatic interaction and H-bond models and was verified by FT-IR and XPS spectroscopy data. We have demonstrated that the nanogenerator made from this DNA-PVDF film shows piezoelectric response to different kinds of mechanical stress such as human finger touches, stepper motor motion, football kicks, and walking. A considerable enhancement of the output voltage is obtained which is dependent on the strength of the periodic mechanical load applied to the nanogenerator. The piezoelectric energy generated can be harvested in charging of capacitors and powering several serially connected LEDs. This flexible piezoelectric energy harvester can potentially serve as power generator for portable electronics.

■ ASSOCIATED CONTENT

Supporting Information

Additional information on XPS, FT-IR measurements, efficiency of NG for capacitor charging and video demonstrating NG responses. The Supporting Information is available free of charge on the ACS Publications website at DOI: 10.1021/acsami.5b04161.

■ AUTHOR INFORMATION

Corresponding Author

*E-mail: dipankar@phys.jdvu.ac.in.

Author Contributions

A.T. and D.M. designed the work and wrote the paper. S.K.G. performed most of the experiments and prepared a report of some analysis in written form. S.G. modeled the PVDF-DNA interaction and performed some experiments. M.M.A.

DOI: 10.1021/acsami.5b04161
ACS Appl. Mater. Interfaces 2015, 7, 16143−16147

performed the NG efficiency calculations and some experiments. K.H. provided valuable comments/suggestions, contributed XPS measurements, and edited the paper. J.H. performed the XAS measurements. D.S. provided the planning of the experimental facilities.

Author Contributions

†A.T. and S.K.G. contributed equally to this work.

Funding

This work was financially supported by a grant from the Science and Engineering Research Board (SERB/1759/2014−15), Government of India.

Notes

The authors declare no competing financial interest.

■ ACKNOWLEDGMENTS

S.K.G. is supported by INSPIRE (ref. No.: IF130865) fellowship. S.G. and M.M.A. are supported by UGC-BSR scheme with ref. no. P-1/RS/79/13 and P-1/RS/191/14, respectively. The help of Guido Beuckert (BTU Cottbus-Senftenberg) in XPS measurements is greatly acknowledged.

■ REFERENCES

(1) Garain, S.; Sinha, T. K.; Adhikary, P.; Henkel, K.; Sen, S.; Ram, S.; Sinha, C.; Schmeißer, D.; Mandal, D. Self-Poled Transparent and Flexible UV-light Emitting Cerium complex-PVDF composite: A High Performance Nanogenerator. *ACS Appl. Mater. Interfaces* **2015**, *7*, 1298−1307.

(2) Adhikary, P.; Garain, S.; Mandal, D. The Co-operative Performance of a Hydrated Salt Assisted Sponge Like P(VDF-HFP) Piezoelectric Generator: An Effective Piezoelectric Based Energy Harvester. *Phys. Chem. Chem. Phys.* **2015**, *17*, 7275−7281.

(3) Yang, Y.; Zhang, H.; Zhu, G.; Lee, S.; Lin, Z. H.; Wang, Z. L. Flexible Hybrid Energy Cell for Simultaneously Harvesting Thermal, Mechanical, and Solar Energies. *ACS Nano* **2012**, *7*, 785−790.

(4) Mao, Y.; Zhao, P.; McConohy, G.; Yang, H.; Tong, Y.; Wang, X. Sponge-Like Piezoelectric Polymer Films for Scalable and Integratable Nanogenerators and Self-Powered Electronic Systems. *Adv. Energy Mater.* **2014**, *4*, 1301624−1301631.

(5) Mandal, D.; Henkel, K.; Schmeißer, D. Improved Performance of a Polymer Nanogenerator Based on Silver Nanoparticles Doped Electrospun P(VDF−HFP) Nanofibers. *Phys. Chem. Chem. Phys.* **2014**, *16*, 10403−10407.

(6) Yang, Y.; Zhang, H.; Chen, J.; Lee, S.; Hou, T. C.; Wang, Z. L. Simultaneously Harvesting Mechanical and Chemical Energies by a Hybrid Cell for Self-powered Biosensors and Personal Electronics. *Energy Environ. Sci.* **2013**, *6*, 1744−1749.

(7) Wen, X.; Yang, W.; Jing, Q.; Wang, Z. L. Harvesting Broadband Kinetic Impact Energy from Mechanical Triggering/Vibration and Water Waves. *ACS Nano* **2014**, *8*, 7405−7412.

(8) Hu, Y. F.; Zhang, Y.; Xu, C.; Zhu, G. A.; Wang, Z. L. High-Output Nanogenerator by Rational Unipolar Assembly of Conical Nanowires and Its Application for Driving a Small Liquid Crystal Display. *Nano Lett.* **2010**, *10*, 5025−5031.

(9) Li, Z.; Zhu, G.; Yang, R.; Wang, A. C.; Wang, Z. L. Muscle-Driven In Vivo Nanogenerator. *Adv. Mater.* **2010**, *22*, 2534−2537.

(10) Wang, L.; Wu, W. Z. Nanotechnology-Enabled Energy Harvesting for Self-Powered Micro-/Nanosystems. *Angew. Chem., Int. Ed.* **2012**, *51*, 11700−11721.

(11) Lovinger, A. J. Ferroelectric Polymers. *Science* **1983**, *220*, 1115−1121.

(12) Martins, P.; Lopes, A. C.; Mendez, S. L. Electroactive Phases of Poly(vinylidene fluoride): Determination, Processing and Applications. *Prog. Polym. Sci.* **2014**, *39*, 683−706.

(13) Sharma, M.; Madras, G.; Bose, S. Process Induced Electroactive β-polymorphs in PVDF: Effect on Dielectric and Ferroelectric Properties. *Phys. Chem. Chem. Phys.* **2014**, *16*, 14792−14799.

(14) Han, H.; Nakagawa, Y.; Takai, Y.; Kikuchi, K.; Tsuchitani, S.; Kosimoto, Y. Microstucture Fabrication on a β-phase PVDF Film by Wet and Dry Etching Technology. *J. Micromech. Microeng.* **2012**, *22* (8), 085030.

(15) Maji, S.; Sarkar, P. K.; Aggarwal, L.; Ghosh, S. K.; Mandal, D.; Sheet, G.; Acharya, S. Self-oriented β-Crystalline Phase in Poly (vinylidene fluoride) Ferroelectric and Piezo-sensitive Ultra-thin Langmuir-Schaefer Film. *Phys. Chem. Chem. Phys.* **2015**, *17*, 8159−8165.

(16) Ke, F.; Luu, Y. K.; Hadjiargyrou, M.; Liang, D. Characterizing DNA Condensation and Conformational Changes in Organic Solvents. *PLoS One* **2010**, *5*, e13308.

(17) Malá, Z.; Kleparnık, K.; Bocek, P. Highly Alkaline Electrolyte for Single-stranded DNA Separations by Electrophoresis in Bare Silica Capillaries. *J. Chromatogr. A* **1999**, *853*, 371−379.

(18) Coates, J. *Interpretation of Infrared Spectra, A Practical Approach in Encyclopedia of Analytical Chemistry*; Meyers, R. A., Ed.; John Wiley & Sons:: Chichester, U.K., 2000; pp 10815−10837.

(19) Yu, L. Y.; Xu, Z. L.; Shen, H. M.; Yang, H. Preparation and Characterization of PVDF-SiO_2 Composite Hollow Fiber UF Membrane by Sol-gel Method. *J. Membr. Sci.* **2009**, *337*, 257−265.

(20) Werling, K. A.; Hutchison, G. R.; Lambrecht, D. S. Piezoelectric Effects of Applied Electric Fields on Hydrogen-Bond Interactions: First-Principles Electronic Structure Investigation of Weak Electrostatic Interactions. *J. Phys. Chem. Lett.* **2013**, *4*, 1365−1370.

(21) Mandal, D.; Kim, K. J.; Lee, J. S. Simple Synthesis of Palladium Nanoparticles, β-Phase Formation, and the Control of Chain and Dipole Orientations in Palladium-Doped Poly (vinylidene fluoride) Thin Films. *Langmuir* **2012**, *28*, 10310−10317.

(22) Sarkar, S.; Garain, S.; Mandal, D.; Chattopadhyay, K. K. Electroactive Phase Formation in PVDF-BiVO4 Flexible Nanocomposite Films for High Energy Density Storage Application. *RSC Adv.* **2014**, *4*, 48220−48227.

(23) Batchelor, D. R.; Follath, R.; Schmeißer, D. Nucl. Instrum. Methods. *Nucl. Instrum. Methods Phys. Res., Sect. A* **2001**, *467-468*, 470−473.

(24) Schmeißer, D.; Hoffmann, P.; Beuckert, G. *Materials for Information Technology*; Zschech, E.; Whelan, C.; Mikolajick, T., Eds.; Springer−Verlag: London, 2005; pp 449−460.

(25) Ohta, T.; Seki, K.; Yokoyama, T.; Morisada, I.; Edamatsu, K. Polarized XANES Studies of Oriented Polyethylene and Fluorinated Polyethylenes. *Phys. Scr.* **1990**, *41*, 150−153.

(26) Stöhr, J. Gomer, R., Eds.; *NEXAFS Spectroscopy*; Springer Series in Surface Science; Springer−Verlag: Berlin, 1996.

(27) Talemi, P.; Delaigue, M.; Murphy, P.; Fabretto, M. Flexible Polymer-on-Polymer Architecture for Piezo/Pyroelectric Energy Harvesting. *ACS Appl. Mater. Interfaces* **2015**, *7*, 8465−8471.

(28) Alam, M. M.; Ghosh, S. K.; Sultana, A.; Mandal, D. Lead-free $ZnSnO_3$/MWCNTs-based Self-powered Flexible Hybrid Nanogenerator for Piezoelectric Power Generation. *Nanotechnology* **2015**, *26* (16), 165403.

(29) Whiter, R. A.; Narayan, V.; Kar-Narayan, S. A. Scalable Nanogenerator Based on Self-Poled Piezoelectric Polymer Nanowires with High Energy Conversion Efficiency. *Adv. Energy Mater.* **2014**, *4*, 1400519.

(30) Joung, M.-R.; Xu, H.; Seo, I.-T.; Kim, D.-H.; Hur, J.; Nahm, S.; Kang, C.-Y.; Yoon, S.-J.; Park, H.-M. Piezoelectric Nanogenerators Synthesized using $KNbO_3$ Nanowires with Various Crystal Structures. *J. Mater. Chem. A* **2014**, *2*, 18547−18553.

DOI: 10.1021/acsami.5b04161
ACS Appl. Mater. Interfaces 2015, 7, 16143−16147